2 Rhodium and iridium

2.1 Introduction

Rhodium and iridium were discovered independently in the same year and also share many resemblances in their chemistry [1–10]. They form a wide range of conventional complexes as well as those of π-bonding ligands. Both metals exhibit an extensive chemistry, principally in the +3 oxidation state, with +1 also being important, and a significant chemistry of iridium +4 existing. Few compounds are known in the +2 state, in contrast to the situation for cobalt, their lighter homologue (factors responsible include the increased stability of the +3 state consequent upon the greater stabilization of the low spin d^6 configuration as 10 Dq increases).

Rhodium was discovered in 1803 by the eminent Norfolk scientist W.H. Wollaston; he dissolved platinum metal concentrates in aqua regia and found that on removing platinum and palladium he was left with a red solution. From this he obtained the salt Na_3RhCl_6, which yielded the metal on reduction with hydrogen. The rose-red colour (Greek rhodon) of many rhodium salts gave the element its name.

In the same year, Smithson Tennant was studying the black aqua regia-insoluble portion of platinum ores and found that, after fusion with soda and extraction with water, the black residue gave a blue solution in hydrochloric acid that went red when heated. The red crystals thus obtained yielded the metal on heating. Tennant gave iridium its name from the Greek iris (rainbow) 'from the striking variety of colours which it gives'.

2.2 The elements and uses

Both rhodium (m.p. 1976°C, b.p. 3730°C) and iridium (m.p. 2410°C, b.p. 4130°C) are unreactive silvery metals, iridium being considerably more dense (22.65 $g\,cm^{-3}$) than rhodium (12.41 $g\,cm^{-3}$), the densest element known apart from osmium. Both form fcc (ccp) lattices and, like the other platinum metals, are ductile and malleable. Neither is affected by aqua regia and they only react with oxygen and the halogens at red heat.

The main use of rhodium is with platinum in catalysts for oxidation of automobile exhaust emissions. In the chemical industry, it is used in catalysts for the manufacture of ethanoic acid, in hydroformylation of alkenes and the synthesis of nitric acid from ammonia. Many applications of iridium rely on

its inertness (e.g. high temperature crucibles, electrode coatings, thermocouples); it is speculated that applications include defence, nuclear and aerospace industries. The inert alloy with osmium is traditionally used in pen nibs.

2.2.1 Extraction

Rhodium and iridium are obtained from the aqua regia-insoluble residues by first smelting with PbO or $PbCO_3$ then treating the product with nitric acid to remove silver along with the lead [11]. The residue is smelted with $NaHSO_4$ which converts the rhodium into soluble $Rh_2(SO_4)_3$, while peroxide fusion of the residues leaves an insoluble residue of IrO_2. Traditionally these products were purified in several stages involving repeated precipitation and solution, ultimately affording the pure salts $(NH_4)_3MCl_6$ (M = Rh, Ir), which then yielded the metal on hydrogen reduction at 1000°C. A more up to date process uses solvent extraction to give a more efficient and rapid separation.

2.3 Halides and halide complexes [3b, 4]

2.3.1 Rhodium halides

Rhodium halides occur mainly in the +3 state. In some cases where a 'soluble' and 'insoluble' form have been reported, the former may be a hydrate.

RhF_3 [12] can be conveniently made by fluorination

$$RhCl_3 \xrightarrow[500°C]{F_2} RhF_3$$

It has the VF_3 structure (Rh–F 1.961 Å) having a hcp array of fluorines with rhodium occupying 1/3 of the octahedral holes. Various hydrates have been reported

$$Rh(NO_2)_6^{3-} \xrightarrow{\text{conc. HF}} RhF_3.9H_2O$$

Insoluble red $RhCl_3$ is made by direct combination, with similar routes for the other trihalides

$$Rh \xrightarrow[800°C]{Cl_2} RhCl_3$$

$$Rh \xrightarrow[\text{then } Br_2\ 400°C]{45\%\ HBr/Br_2,\ \text{heat}} RhBr_3\ (\text{red})$$

$$Rh \xrightarrow[400°C]{I_2} RhI_3\ (\text{black})$$

All of these probably have the $AlCl_3$ structure (unconfirmed for RhI_3) with bond lengths (EXAFS) of 2.337 Å (Rh–Cl) [13] and 2.48 Å (Rh–Br) [14]. 'Soluble' chlorides and bromides are made by dissolving the oxide in the appropriate acid.

Rhodium trihalides (and complexes like K_3RhBr_6) are frequently added to photographic emulsions in trace quantities to improve the gradation of the emulsion (the 'rhodium effect') [15].

Only fluorides are known in higher oxidation states with tetra-, penta- and hexafluorides isolated.

$$RhBr_3 \xrightarrow{BrF_3} RhF_4.2BrF_3 \xrightarrow{\text{heat}} RhF_4$$

$$Rh \xrightarrow[400°C,\,6\,atm]{F_2} RhF_5$$

$$RhF_3 \xrightarrow[400°C]{F_2} RhF_5$$

$$RhF_5 \xrightarrow[250°C,\,30\,atm]{F_2} RhF_6$$

Little is known about the structure of purple paramagnetic RhF_4 ($\mu_{eff} = 1.1\,\mu_B$) but it may be similar to PdF_4 [16]. RhF_5 has a tetrameric structure [17] similar to RuF_5 and OsF_5 (section 1.3.4); the terminal Rh–F bonds are 1.808 Å and the bridges 2.01 Å. The ruby red solid (m.p. 95.5°C) has $\mu_{eff} = 2.39\,\mu_B$. Rhodium hexafluoride is a very reactive black solid (attacking glass at room temperature) vaporizing to a deep brown gas (triple point *c.* 70°C). EXAFS measurements indicate a Rh–F bond length of 1.838 Å [18].

Various ill-defined binary halides have been reported but not characterized, such as RhI_2.

2.3.2 Iridium halides

The pattern of iridium halides resembles rhodium, with the higher oxidation states only represented by fluorides. The instability of iridium(IV) halides, compared with stable complexes $IrCl_4L_2$ and the ions IrX_6^{2-} (X = Cl, Br, I), though unexpected, finds parallels with other metals, such as plutonium.

Preparations of the halides include [19]

$$IrF_4 \xrightarrow{400°C} IrF_3\,(\text{black})$$

$$IrF_5 + SF_4 \xrightarrow{400°C} IrF_3 + SF_6$$

$$Ir \xrightarrow[600°C]{Cl_2} \alpha\text{-}IrCl_3\,(\text{brown}) \xrightarrow[\text{vacuum}]{750°C} \beta\text{-}IrCl_3\,(\text{deep red})$$

$$Ir \xrightarrow[540°C,\,8-9\,atm]{Br_2\,(sealed\,tube)} IrBr_3\,(yellow)$$

$$Ir(OH)_3 \xrightarrow[2.\,heat,\,400°C]{1.\,HI\,20°C} IrI_3\,(black)$$

$$Ir + 2IrF_6 \xrightarrow{1\,to\,15\,torr} 3IrF_4\,(red-brown)\,[20]$$

$$2Ir + 5F_2 \xrightarrow{350-380°C} 2IrF_5\,(yellow-green)$$

$$Ir + 3F_2 \xrightarrow{240°C} IrF_6\,(yellow)$$

All the trihalides are known to have 6-coordinate iridium (except the unknown structure of IrI_3). IrF_3 has the PdF_3 structure; α-$IrCl_3$ and $IrBr_3$ have structures of the $AlCl_3$ type (Ir–Cl 2.30–2.39 Å in the former).

IrF_5 (until 1965 thought to be IrF_4) is paramagnetic ($\mu = 1.32\,\mu_B$) and has the same tetrameric structure as RhF_5; it has a slightly higher m.p. (104°C) than IrF_6, in keeping with the larger molecular units [21]. Like RhF_6, IrF_6 is very reactive, attacking most glass and undergoing slow photolysis to IrF_5. IrF_6 has a regular octahedral structure in the vapour (Ir–F 1.83 Å) and in the solid state (Ir–F 1.822 Å, EXAFS). It is paramagnetic with $\mu \sim 3\,\mu_B$; vibrational frequencies of the octahedral molecule have been assigned to bands at 719 cm^{-1} (T_{1u}), 701.7 cm^{-1} (A_{1g}) and 645 cm^{-1} (E_g) [18, 22].

2.3.3 Halometallates

A wide range of MX_6^{n-} species exist, typical preparations appear below.

$$RhF_3 \xrightarrow[550°C]{KF,\,CsF} Cs_2KRhF_6\,(pink)$$

$$RhCl_3.3H_2O \xrightarrow[3M\,HCl]{ACl} A_3RhCl_6.H_2O \xrightarrow{heat} A_3RhCl_6\,(red)\,(A = K, Rb, Cs)$$

$$Rh(OH)_3 \xrightarrow[KBr]{HBr} K_3RhBr_6$$

$$RhF_3 \xrightarrow[NaCl]{BrF_3} Na_2RhF_6\,(yellow)$$

$$RhF_6 \xrightarrow[25°C]{NOF} (NO)_2RhF_6\,(yellow)$$

$$Cs_3RhCl_6 \xrightarrow{Cl_2\,or\,Ce^{4+}} Cs_2RhCl_6\,(dark\,green)$$

$$RhF_5 \xrightarrow[HF\,or\,IF_5,\,20°C]{MF} MRhF_6\,(yellow\text{-}ochre)\,(M = K, Cs)$$

$$M_2IrF_6 \xrightarrow[MF]{N_2H_4} M_3IrF_6\,(M = K, Rb, Cs)$$

$$Ir \xrightarrow[KCl]{Cl_2} K_2IrCl_6 \xrightarrow[80°C]{C_2O_4^{2-}} K_3IrCl_6.H_2O \text{ (yellow)}$$

$$M_3IrCl_6 \xrightarrow[H_2O]{HBr} M_3IrBr_6.H_2O \text{ (green)}$$

$$Cs_3IrBr_6 \xrightarrow[160°C]{NaI} Cs_3IrI_6 \text{ (brown)}$$

$$MIrF_6 \xrightarrow{H_2O} M_2IrF_6 + IrO_2 + O_2 \text{ (M = alkali metal)}$$

$$IrO_2.nH_2O \xrightarrow[HBr]{MBr} M_2IrBr_6 \text{ (purple)}$$

$$IrBr_3 \xrightarrow[BrF_3]{KBr} KIrF_6 \text{ (white)}$$

$$IrF_6 \xrightarrow{NOF/F_2} NO^+IrF_6^-$$

IrI_6^{2-} does not exist: Ir^{4+} is too strongly oxidizing to coexist with the reducing I^-.

Points to note in these syntheses include the use of BrF_3 as an oxidizing agent, and the stability of IrX_6^{2-}, also used as a source of IrX_6^{3-}.

Structural data [23] (Table 2.1) confirm the presence of the hexahaloanions in these states; M_2RhF_7 (M = Sr, Pb) contain RhX_6^{3-} octahedra too, as do salts like $(MeNH_3)_4RhX_7$ (X = Cl, Br) and $(enH_2)_2RhX_7$.

Many of the compounds in higher oxidation states are reactive, and for moisture-sensitive solids that cannot be crystallized, some of the bond lengths quoted in Table 2.1 are from EXAFS measurements [24]. Raman spectroscopy is likewise well suited to studying such reactive compounds, and vibrational data for halometallates are given in Table 2.2; trends illustrated include the decrease in frequency as the oxidation state of the metal decreases, and similarly a decrease in vibrational frequency, for a given oxidation state, with increasing mass of the halogen.

Table 2.1 Bond lengths in hexahalometallate ions and related species

Rhodium	Rh–X (Å)	Iridium	Ir–X (Å)
RhF_6	1.838	IrF_6	1.822
RhF_6^-	1.855	IrF_6^-	1.910
RhF_6^{2-}	1.934	IrF_6^{2-}	1.928
RhF_6^{3-}	1.969		
$RhCl_6^{2-}$	2.313	$IrCl_6^{2-}$	2.332
$RhCl_6^{3-}$	2.330–2.354	$IrCl_6^{3-}$	2.327–2.387
		$IrBr_6^{2-}$	2.515–2.549
$RhBr_6^{3-}$	2.465–2.485	$IrBr_6^{3-}$	2.486–2.512

Table 2.2 Vibrational fundamentals in MX_6^{n-} species (cm^{-1}) (M = Rh, Ir; X = F, Cl, Br, I; $n = 0$–3)

	$\nu_1(A_{1g})$	$\nu_3(T_{1u})$		$\nu_1(A_{1g})$	$\nu_3(T_{1u})$
RhF_6			IrF_6	702	719
RhF_6^-	632	655	IrF_6^-	671	
RhF_6^{2-}	592		IrF_6^{2-}	603–610	554
RhF_6^{3-}			IrF_6^{3-}		
$RhCl_6^{2-}$	320	335	$IrCl_6^{2-}$	345–346	313–321
$RhCl_6^{3-}$	302–308	312	$IrCl_6^{3-}$	330	296
			$IrBr_6^{2-}$	215	221
$RhBr_6^{3-}$	187–190	244-260	$IrBr_6^{3-}$	198	209
			IrI_6^{3-}	149	175

The hexahalometallate(III) ions are reasonably stable, except for IrI_6^{3-}; water-sensitive Cs_3IrI_6 was made by tempering pellets of Cs_3IrBr_6 and NaI at 160°C for some days [25]. As expected for low-spin d^6 systems, these are diamagnetic, but the MX_6^{2-} species are paramagnetic with one unpaired electron [26]. Thus Cs_2RhCl_6 has $\mu_{eff} = 1.7\,\mu_B$ and various RhF_6^{2-} salts have moments of *c.* $2.0\,\mu_B$; moments in this range have been reported for IrX_6^{2-} (X = F, Cl, Br).

Salts of $IrCl_6^{2-}$ were used in the classic first ESR experiments to demonstrate delocalization of unpaired electrons onto the chloride ligand (Figure 2.1); the unpaired electron spends 30% or more of its time in ligand orbitals in this case [27].

Na_2IrCl_6 is a convenient starting material in the synthesis of iridium compounds.

$NaRhF_6$ is reported to have $\mu = 2.8\,\mu_B$.

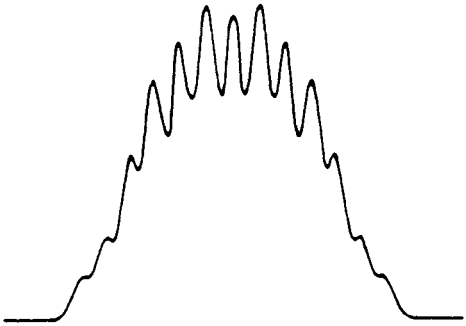

Figure 2.1 Ligand hyperfine structure in the ESR spectrum of $Na_2[(Ir, Pt)Cl_6].6H_2O$. (Reproduced with permission from *Proc. R. Soc., London, Ser. A*, 1953, **219**, 526.)

Mixed halometallates [28] can be synthesized: $RhCl_6Br_{6-x}^{3-}$ from the reaction of $RhCl_6^{3-}$ with HBr, or $RhBr_6^{3-}$ with HCl. Individual isomers have been identified in solution by ^{103}Rh NMR, which can even distinguish between stereoisomers (Figure 2.2) and shows isotopic splitting (Figure 2.3).

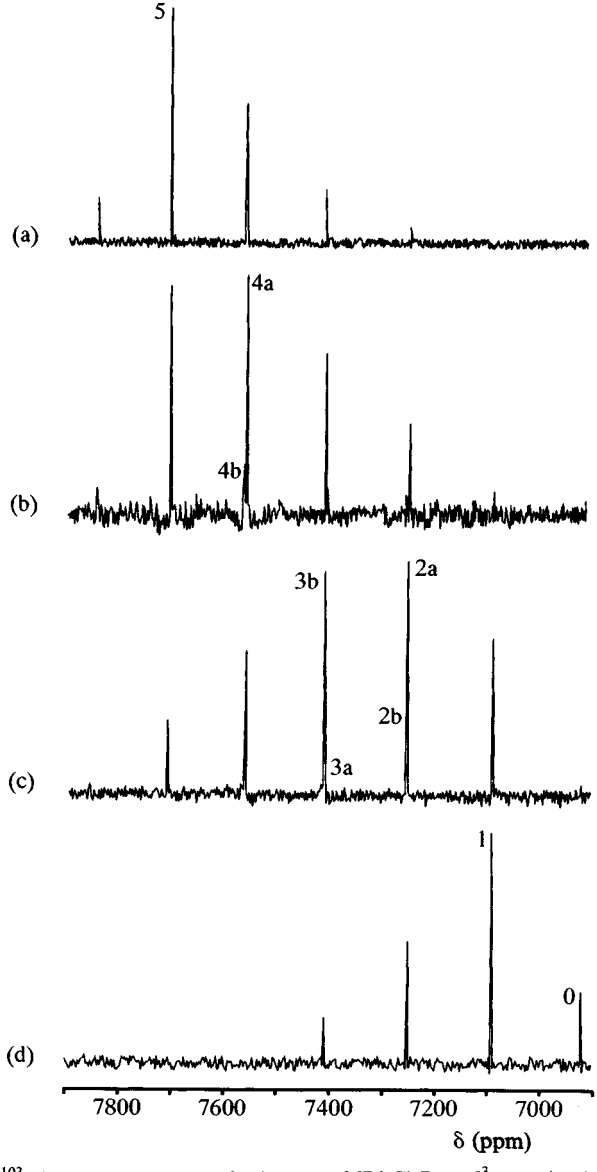

Figure 2.2 ^{103}Rh NMR spectrum of mixtures of $[RhCl_nBr_{6-n}]^{3-}$ species ($n = 0$–6; a denotes *cis,fac*-isomer, b denotes *trans,mer*-isomer). (a–d) are varying Cl:Br ratios in the starting material. (Reproduced with permission from *Z. Naturforsch., Teil B*, 1989, **44**, 1402.)

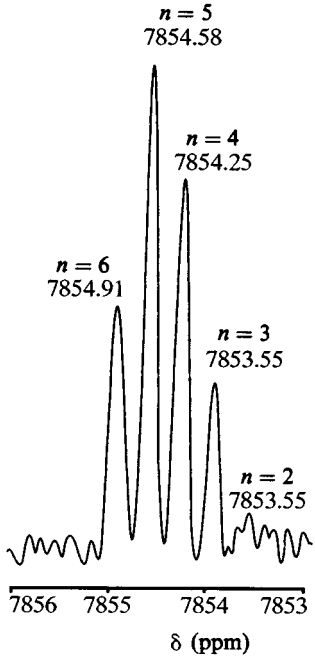

Figure 2.3 ^{103}Rh NMR spectrum of mixtures of $[Rh^{35}Cl_n^{37}Cl_{6-n}]^{3-}$ species ($n = 2$–6). (Reproduced with permission from *Z. Naturforsch., Teil B*, 1989, **44**, 1402.)

The series $[IrX_{6-x}Cl_x]^{2-}$ have likewise been made, as have the free acids $(H_3O)_2IrX_6$ (X = Cl, Br).

Various dinuclear complexes exist

$$A_3RhCl_6 \xrightarrow{H_2O} A_2RhCl_5(H_2O) \xrightarrow{\text{heat}} A_3Rh_2Cl_9$$

(A = alkali metal)

$$2RhX_6^{3-} + 6Bu_4N^+ \xrightarrow[(X=Cl, Br)]{CH_2Cl_2} (Bu_4N)_3Rh_2X_9 + 3Bu_4NX$$

In the latter example, the ligand abstraction is favoured by the non-polar solvent CH_2Cl_2. IR spectra distinguish between the bridging and terminal groups; thus in $Cs_3Rh_2X_9$, terminal Rh–X stretching vibrations occur in the regions 342–361 cm^{-1} (X = Cl) and 252–272 cm^{-1} (X = Br) with bridging Rh–X vibrations in the regions 267–302 cm^{-1} (X = Cl) and 171–195 cm^{-1} (X = Br) [29].

2.4 Oxides, hydrides and other binary compounds

Both rhodium and iridium form the oxides M_2O_3 and MO_2 [30]. Heating

rhodium in air or oxygen (300–1000°C) yields brown Rh_2O_3, also obtained by heating rhodium nitrate at 730°C.

$$4Rh(NO_3)_3.6H_2O \rightarrow 2Rh_2O_3 + 12NO_2 + 3O_2 + 24H_2O$$

It exists in two stable forms, of which the α-form has the corundum (α-Al_2O_3) structure with octahedrally coordinated rhodium (Rh–O 2.03–2.07 Å); the β-form and a high-temperature form also have octahedral coordination. Black RhO_2 has the rutile structure (Rh–O 1.95–1.97 Å) and is best made by heating rhodium or Rh_2O_3 at 400–900°C under oxygen pressures up to 3500 atm.

Ir_2O_3 can be made by heating K_2IrCl_6 with Na_2CO_3; it is a (impure) brown solid about which little is known. Like RhO_2, IrO_2 also has the rutile structure. It is obtained by heating the metal in oxygen or by dehydrating the hydrated oxide precipitated on hydrolysis of Ir^{4+}(aq.)

The oxides decompose on heating:

$$2Ir_2O_3 \xrightarrow{500°C} Ir + 3IrO_2$$

$$IrO_2 \xrightarrow{1100°C} Ir + O_2$$

$$4RhO_2 \xrightarrow{680°C} 2Rh_2O_3 + O_2.2Rh_2O_3 \xrightarrow{1050°C} 4Rh + 3O_2$$

Rhodium(III) hydroxide is an ill-defined compound $Rh(OH)_3.nH_2O$ ($n \sim 3$) obtained as a yellow precipitate by careful addition of alkali to Na_3RhCl_6. Addition of imidazole solution to suitable aqua ions leads to the precipitation of 'active' rhodium(III) hydroxides formulated as $Rh(OH)_3(H_2O)_3$, $Rh_2(\mu\text{-}OH)_2(OH)_4(H_2O)_4$ and $Rh_3(\mu\text{-}OH)_4(OH)_5(H_2O)_5$ [31]. Hydrated iridium(III) hydroxide is obtained as a yellow precipitate from Ir^{3+} (aq.) at pH 8.

The metals form the usual wide range of binary compounds. Therefore, a range of sulphides and selenides are known, including MX_2 (M = Rh, Ir; X = S, Se, Te), M_3X_8 (X = S, Se), M_2S_3 and IrS_3. Of these, M_2S_3 is isostructural, containing pairs of face-sharing octahedra linked into a three-dimensional array by further sharing of sulphur. $RhSe_2$ and IrX_2 (X = S, Se) contain a special variety of the pyrite structure and are probably both represented as $M^{3+}X^{-1.5}(X_2^{3-})_{1/2}$ [32].

Other binary compounds include MAs_3 (M = Rh, Ir), which has the skutterudite ($CoAs_3$) structure [33] containing As_4 rectangular units and octahedrally coordinated M. The corresponding antimonides are similar. M_2P (M = Rh, Ir) has the anti-fluorite structure while MP_3 has the $CoAs_3$ structure. In another compound of this stoichiometry, $IrSi_3$, 9-coordination exists for iridium.

No binary hydrides have been characterized, but reactions of the metal powders with alkali metal hydrides in a hydrogen atmosphere lead to Li_3RhH_4 (planar RhH_4^{3-}) and M_3MH_6 (M = Li, Na; M = Rh, Ir) with octahedral MH_6^{3-} [34].

2.5 Aqua ions and simple salts

Aqua ions and simple salts have been thoroughly investigated recently [35]. Rhodium perchlorate, $Rh(ClO_4)_3.6H_2O$, can be made as yellow crystals by dissolving rhodium hydroxide in perchloric acid or alternatively by repeatedly heating hydrated rhodium chloride with perchloric acid. (Equilibrium is only slowly established and oligomers persist in quite acid solutions.) It contains slightly distorted $Rh(H_2O)_6^{3+}$ octahedra (Rh–O 2.128–2.136 Å); the Rh–O bonds may be lengthened slightly compared with the alum by hydrogen bonding to perchlorate ions. Solutions of iridium(III) perchlorate have been made by hydrolysis of $(NH_4)_2IrCl_6$, reacting the hydrolysis product with $HClO_4$ and then removing polymeric species by ion exchange. The alums also contain the hexaqua ion:

$$M(OH)_3 \xrightarrow{H_2SO_4} M_2(SO_4)_3(aq.) \xrightarrow{Cs_2SO_4} CsM(SO_4)_2.12H_2O$$

M–O bond lengths are 2.016 Å (Rh) and 2.041 Å (Ir), the former corresponds well to the value of 2.04 Å deduced from X-ray studies on aqueous solutions of $Rh(H_2O)_6^{3+}$ [36].

$Rh(H_2O)_6^{3+}$ is quite acidic ($pK_a = 3.4$ at 25°C). Spectroscopic study of crystals of the alums at 80 K leads to the assignment of ν_1 (A_{1g}) in $M(OH_2)_6^{3+}$ to bands at 548 cm^{-1} (Rh) and 553 cm^{-1} (Ir); in solution at room temperature they are found at 529 and 536 cm^{-1}, respectively.

Brown rhodium nitrate is reportedly formed from the reaction of RhI_3 with boiling nitric acid; it forms a hexahydrate.

The rhodium(II) aqua ion is not yet completely characterized. Cr^{2+} reduction of $Rh(H_2O)_5Cl^{2+}$ gives a diamagnetic species believed to be Rh_2^{4+} (aq.) [37], which may have the structure $(H_2O)_4Rh(\mu\text{-}OH_2)_2Rh(H_2O)_4^{4+}$.

In addition to the aqua ion, a range of mixed aquo–halo complexes are known [38], including all 10 isomers of $Rh(H_2O)_{6-x}Cl_x^{(3-x)+}$. Synthetic entry into the series is possible from either end, the determining factor being the labilizing effect of chloride:

$$Rh(H_2O)_6^{3+} \xrightarrow{Cl^-} RhCl(H_2O)_5^{2+} \xrightarrow{Cl^-} \textit{trans}\text{-}RhCl_2(H_2O)_4^+$$

$$\xrightarrow{Cl^-} \textit{mer}\text{-}RhCl_3(H_2O)_3$$

$$RhCl_6^{3-} \xrightarrow{H_2O} RhCl_5(H_2O)^{2-} \xrightarrow{H_2O} \textit{cis}\text{-}RhCl_4(H_2O)^-$$

$$\xrightarrow{H_2O} \textit{fac}\text{-}RhCl_3(H_2O)_3$$

This affects both the position of substitution and the rate; thus $RhCl(H_2O)_5^{2+}$ substitutes more than an order of magnitude faster than $Rh(H_2O)_6^{3+}$. These substitutions are all believed to follow a dissociative (S_N1) reaction. Particular compounds can sometimes be obtained under specific conditions;

thus recrystallizing a $RhCl_6^{3-}$ salt generally affords the corresponding $RhCl_5(H_2O)^{2-}$ species. Usually a mixture is formed, needing to be separated by ion-exchange: on refluxing $Rh(H_2O)_6(ClO_4)_3$ in 0.5 M HCl for 6–8 h, *mer*-$RhCl_3(H_2O)_3$ is the dominant product, while 15 min reflux of K_3RhCl_6 in dilute $HClO_4$ gives principally *fac*-$RhCl_3(H_2O)_3$. Individual species afford separate peaks in their electronic and vibrational spectra but in a mixture these will tend to overlap. However, separate signals can be seen in the ^{103}Rh NMR spectrum of such a mixture, it is even possible to discern isotopic splitting (see also Figure 2.3) [39].

Similar studies have been carried out on the corresponding bromides. Some structures have been determined; in Me_4N^+ [*trans*-$RhCl_4(H_2O)_2]^-$, Rh–O is 2.032 Å while Rh–Cl distances average 2.33 Å. $(NH_4)_2RhCl_5(H_2O)$ has Rh–O of 2.090 Å, *cis*-Rh–Cl distances average 2.347 Å while Rh–Cl *trans* to O is 2.304 Å (*trans*-influence of Cl); in the corresponding Cs salt, these distances are 2.096, 2.337 and 2.300 Å, respectively [40]. In *trans*-$[Ir(H_2O)_4Cl_2]^+$, Ir–Cl is 2.350 Å and Ir–O 2.039–2.048 Å.

2.6 Compounds of rhodium(0)

The best defined rhodium(0) compound [41] is diamagnetic $Rh_2(PF_3)_8$

$$RhCl_3 \xrightarrow[150°C,\,250\,atm]{PF_3/Cu} Rh_2(PF_3)_8$$

It is believed to be metal–metal bonded $(PF_3)_4Rh-Rh(PF_3)_4$ and readily reacts with hydrogen

$$Rh_2(PF_3)_8 + H_2 \rightarrow 2RhH(PF_3)_4$$

Electrochemical reduction in MeCN of various $RhCl(R_3P)_3$ complexes give the diamagnetic $Rh(R_3P)_4$ ($R_3P = Ph_3P$, Me_2PhP), which are probably analogous to the PF_3 complex.

2.7 Compounds of rhodium(I)

Many important compounds are found in the +1 oxidation state [42], though unlike rhodium(III) it has no aqueous chemistry. Rhodium(I) generally forms 4-coordinate square planar and 5-coordinate species, the latter being the highest CN expected for the d^8 configuration under the 18-electron rule. (An octahedral rhodium(I) complex would involve putting two electrons in an anti-bonding orbital, as well as more steric crowding.)

2.7.1 *Tertiary phosphine complexes*

Tertiary phosphine complexes [42] are the most important rhodium(I) compounds. $RhCl(PPh_3)_3$ ('Wilkinson's compound'), a hydrogenation catalyst, is the most important, but they exist in a range of stoichiometries.

Synthesis follows several routes:

1. Substitution in rhodium(I) alkene complexes

$$RhCl_3.3H_2O \xrightarrow{C_2H_4} [RhCl(C_2H_4)_2]_2 \xrightarrow{PR_3} RhCl(PR_3)_3 \qquad (R = \text{alkyl})$$

$$RhF(C_8H_{12})_2 \xrightarrow{Pcy_3} RhF(Pcy_3)_2 \xrightarrow{NaX} RhX(Pcy_3)_2$$

$$[RhCl(C_8H_{12})_2]_2 \xrightarrow{P(OMe)_3} [RhCl\{P(OMe)_3\}_2]_2$$

2. Displacement of CO, only possible with strong π-acids

$$[RhCl(CO)_2]_2 \xrightarrow{PF_3} [RhCl(PF_3)_2]_2$$

3. Substitution of other phosphines

$$RhCl(PPh_3)_3 \xrightarrow[PMe_3]{\text{exc.}} [Rh(PMe_3)_4]^+Cl^-$$

4. Reduction using certain arylphosphines as reducing agents

$$RhCl_3.3H_2O \xrightarrow[EtOH/boil]{\text{exc. } PPh_3} RhCl(PPh_3)_3$$

2 : 1 complexes

The intensely reactive $RhX(Pcy_3)_2$ complexes are probably monomers; they bind both N_2 and SO_2 [43a], but most $RhX(PR_3)_2$ systems are dimers (R = Ph, X = Cl, OH; X-ray [43b]) (Figure 2.4)

$$[RhCl(PPr^i_3)_2]_2 + 2L \rightarrow 2RhClL(PPr^i_3)_2 \qquad (L = H_2, CO, Bu^tNC)$$

where the bridge can be cleaved

$$[RhCl(PPh_3)_2]_2 + 2PPh_3 \rightarrow 2RhCl(PPh_3)_3$$

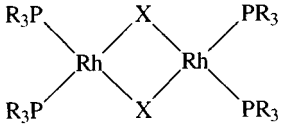

X	Rh–X	Rh–P	Rh–Rh
Cl	2.40	2.200–2.213	3.662
OH	2.06	2.185–2.207	3.278

Figure 2.4 Bond lengths in $[Rh(PPh_3)_2X]_2$ dimers.

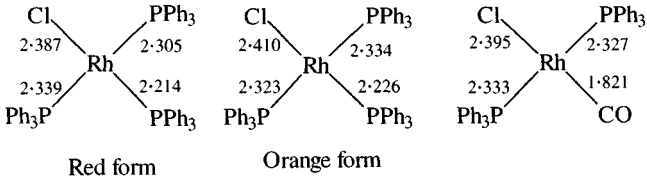

Figure 2.5 Bond lengths in $Rh(X)Cl(PPh_3)_2$ (X = CO, PPh_3).

3 : 1 complexes

A wide range of $RhX(QR_3)_3$ complexes exist (QR_3, e.g. PMe_3, PMe_2Ph, PPh_3, $AsPh_3$, etc.), generally made by replacing alkenes. Red $RhCl(PPh_3)_3$ [44] is made by an unusual route

$$RhCl_3 + 4PPh_3 \xrightarrow[EtOH]{\text{reflux}} RhCl(PPh_3)_3 + Ph_3PO$$

The ability of triphenylphosphine to act as a reducing agent probably involves initial formation of Ph_3PCl_2, which then undergoes solvolysis. If the synthesis is carried out using a small volume of ethanol, an orange polymorph is formed [45].

The crystal structures of both forms of $RhCl(PPh_3)_3$ show square planar coordination geometry (with a slight tetrahedral distortion). The mutually *trans* Rh–P bonds are similar to those in the less congested $RhCl(CO)(PPh_3)_2$, suggesting that steric crowding is not responsible for this distortion, which is also found in $RhCl(PMe_3)_3$ (Figure 2.5).

There are, however, short Rh–H contacts (2.77–2.84 Å) to *ortho*-hydrogens in phenyl groups. The Rh–P bond *trans* to Cl is some 0.1 Å shorter than the others, evidence of the weak *trans*-influence of chloride [46].

The ^{31}P NMR spectrum in solution [47] is in accordance with a square planar structure (Figure 2.6).

It shows a doublet of doublets owing to the pair of equivalent phosphorus nuclei, the signal being split by coupling to ^{103}Rh ($I = \frac{1}{2}$) and to the unique phosphorus; similarly the resonance owing to the third phosphorus shows coupling to two equivalent phosphorus nuclei, the resulting triplet being

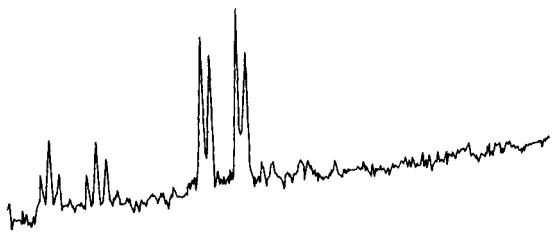

Figure 2.6 The ^{31}P NMR spectrum of $RhCl(PPh_3)_3$ at 30°C in C_6H_6 solution. (Reprinted with permission from *J. Am. Chem. Soc.*, 1972, **94**, 340. Copyright (1972) American Chemical Society.)

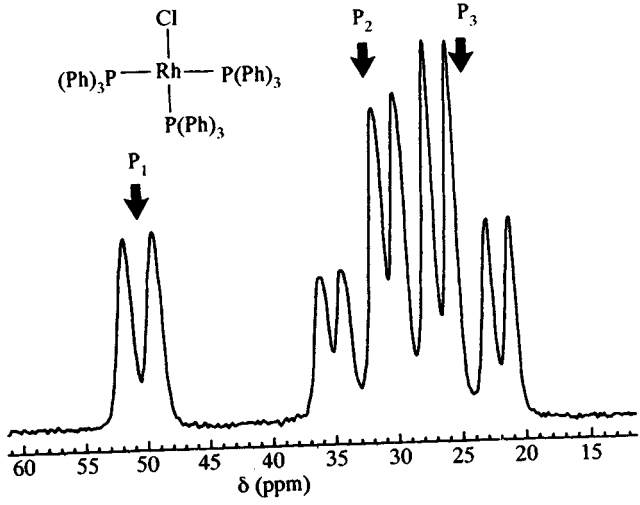

Figure 2.7 The solid-state ^{31}P NMR spectrum of $RhCl(PPh_3)_3$. (Reprinted with permission from *Organometallics*, 1992, **11**, 3240. Copyright (1992) American Chemical Society.)

split by coupling to rhodium. The solid-state ^{31}P NMR spectrum (Figure 2.7) is composed of a low-field cluster owing to the unique phosphorus split by coupling with rhodium (*cis*-P–P coupling is too small to be resolved); the multiplet has been analysed as the AB part of an ABX system, showing the two *trans*-phosphines are non-equivalent in the solid state.

$RhCl(PPh_3)_3$ is an air-stable solid (m.p. 157°C) soluble in a wide range of organic solvents with little dissociation of ligands. It does react readily with dioxygen in solution [48] forming a number of O_2 adducts (Figure 2.8); the consequent dissociation of PPh_3 is probably the reason why molecular weight measurements in incompletely deoxygenated solvents have implied

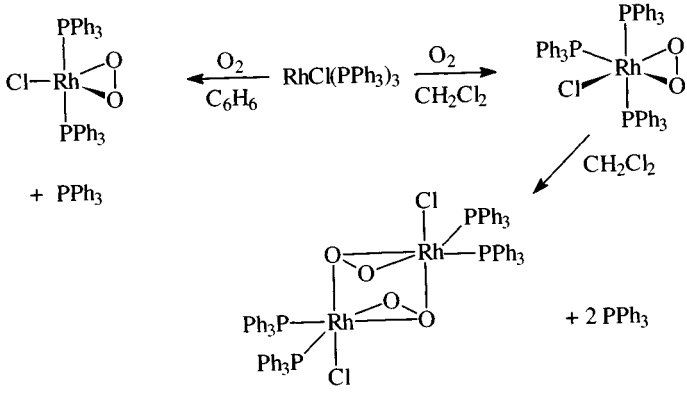

Figure 2.8 Rhodium dioxygen complexes.

dissociation for $RhCl(PPh_3)_3$. (It is notable that the isoelectronic 16-electron $Pt(PPh_3)_3$ shows no significant dissociation in solution.)

$RhCl(PPh_3)_3$ is a very active homogenous hydrogenation catalyst, because of its readiness to engage in oxidative addition reactions with molecules like H_2, forming Rh–H bonds of moderate strength that can subsequently be broken to allow hydride transfer to the alkene substrate. A further factor is the lability of the bulky triphenylphosphines that creates coordinative unsaturation necessary to bind the substrate molecules [44].

Reactions of $RhCl(PPh_3)_3$ can be divided into three classes (Figure 2.9)

1. oxidative addition (usually involving partial loss of PPh_3)
2. halide substitution
3. substitution of PPh_3 ligands (whole or partial).

In class (1), a range of small molecules adds to rhodium, usually with the loss of one PPh_3, thus maintaining the 16-electron configuration, rather than an 18-electron species unable to bind a substrate.

The reversible addition of hydrogen is the most significant of these reactions. In the presence of excess PPh_3, $RhH_2Cl(PPh_3)_3$ is formed, but generally the 5-coordinate $RhHCl_2(PPh_3)_2$ is obtained. Chlorine and HCl likewise add with fission of the X–Cl bond and loss of one PPh_3; $RhHCl_2(PPh_3)_2$ will insert ethene to form an ethyl complex.

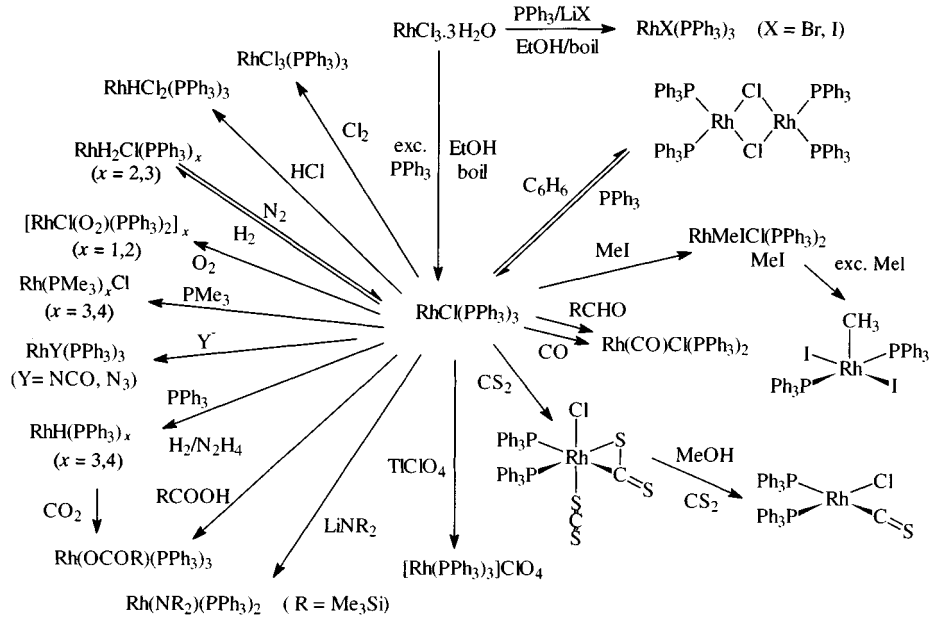

Figure 2.9 Synthesis and reactions of $RhCl(PPh_3)_3$.

The reaction with MeI proceeds in two stages. Initial reaction is oxidative addition to give a rhodium(III) species, isolated as a MeI adduct

$$RhCl(PPh_3)_3 + 2MeI \rightarrow RhClIMe(PPh_3)_2MeI + PPh_3$$

This then eliminates MeCl on recrystallization from benzene

$$RhClIMe(PPh_3)_2(MeI) \rightarrow MeCl + RhI_2(Me)(PPh_3)_2$$

Replacement reactions frequently involve a simple substitution of halide by an anionic ligand (e.g. N_3, NCO, S_2CNR_2). While chloride can be replaced by bis(trimethylsilyl)amide, $N(SiMe_3)_2$, most alkylamides are unstable to α-hydride elimination, forming the hydride $RhH(PPh_3)_3$ [49] (which is also obtained in the attempted preparation of $Rh(CH_2CH_2Me)((PPh_3)_3)$. The hydride ligand can be identified in the ^1H NMR spectrum of $RhH(PPh_3)_3$ by its high-field line (doublet, $\delta = -8.3$ ppm, $J(Rh-H) = 12.4$ Hz). The ^{31}P NMR spectrum at room temperature is a doublet ($J(Rh-P)$ 164 Hz) but on cooling a fluxional process slows down and the spectrum converts into a double doublet and a double triplet (Figure 2.10) that overlap slightly.

The double triplet results from the unique phosphorus, split into a triplet by interaction with two equivalent phosphorus atoms ($J(P-P)$ 25 Hz) then split into a doublet by rhodium ($J(Rh-P)$ 145 Hz).

The double doublet corresponds to P_B, with splitting owing to phosphorus A (*cis*) ($J(P-P)$ 25 Hz) and rhodium ($J(Rh-P)$ 172 Hz). The fluxional behaviour is consistent with a rapidly rearranging (at room temperature) square planar structure rather than a tetrahedral one (Figure 2.11).

Determination of this crystal structure of the complex did not locate the hydride ligand but its position can be deduced from the distortion from

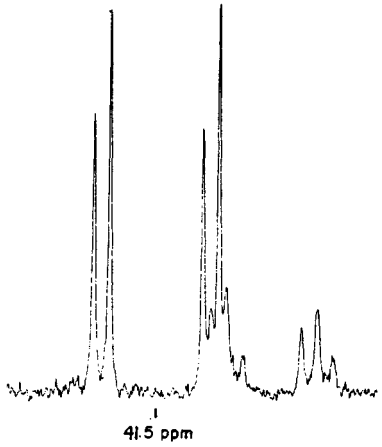

Figure 2.10 ^{31}P NMR spectrum of $RhH(PPh_3)_3$. (Reprinted with permission *Inorg. Chem.*, 1978, **17**, 3066. Copyright (1978) American Chemical Society.)

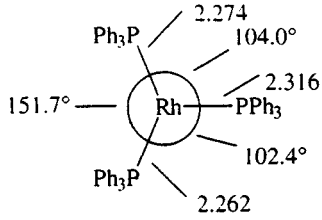

Figure 2.11 Bond lengths in $RhH(PPh_3)_3$ (hydride not shown).

regular trigonal geometry and the lengthened Rh–P bond *trans* to hydride. ($RhH(PPh_3)_4$, however, has a regular RhP_4 core so that here hydride has no stereochemical influence.)

Alkylation of $RhCl(PPh_3)_3$ yields unstable alkyls that undergo CO_2 insertion; $Rh(OCOPh)(PPh_3)_3$ has monodentate benzoate (X-ray).

Halide abstraction in donor solvents (with e.g. $TlClO_4$) affords [50] pseudo-tetrahedral $[Rh(solvent)(PPh_3)_3]^+$ ions (solvent, e.g. MeCN, Me_2CO, ROH) (Figure 2.12), which on recrystallization from CH_2Cl_2 gives $Rh(PPh_3)_3^+ClO_4^-$ (Figure 2.13) [51].

This has a distorted trigonal planar (nearly T-shaped) geometry with weak Rh–C and Rh–H interactions owing to the close approach of a phenyl group (Rh–H 2.56 Å, Rh–C 2.48 Å) supplementing the three Rh–P bonds in what is formally a 14-electron species. This ion is also formed by protonation of $RhH(PPh_3)_4$ (note the hydride ligand behaving as H^-).

$$RhH(PPh_3)_4 \xrightarrow{H_2C(SO_2CF_3)_2} [Rh(PPh_3)_3]^+HC(SO_2CF_3)_2^- + H_2 + PPh_3$$

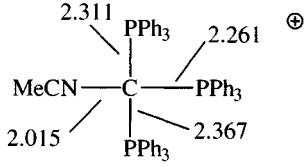

Figure 2.12 Bond lengths in $[Rh(MeCN)(PPh_3)_3]^+$.

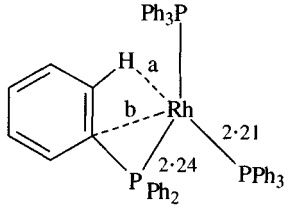

Figure 2.13 Bond lengths in $[Rh(PPh_3)_3]^+ClO_4^-$ showing short Rh–H and R–C contacts. a = 2.56 Å; b = 2.48 Å.

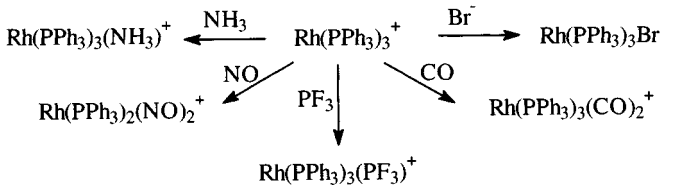

Figure 2.14 Reactions of $[Rh(PPh_3)_3]^+$.

^{31}P NMR spectra indicate the T-shape geometry is retained in solution at −30°C but that the molecule is fluxional at room temperature. $Rh(PPh_3)_3^+$ undergoes a range of addition reactions with Lewis bases (CO, PF_3, NH_3) to afford various 16- and 18-electron species (Figure 2.14).

Substitution reactions of $RhCl(PPh_3)_3$ where PPh_3 is completely displaced are relatively rare, though this is achieved with PMe_3, affording $Rh(PMe_3)_3Cl$ and $Rh(PMe_3)_4^+Cl^-$. More usually, as with CO, DMSO and C_2H_4, one phosphine is displaced; indeed the stability of *trans*-$RhCl(CO)(PPh_3)_2$ is such that aldehydes are decarbonylated by $RhCl(PPh_3)_3$. The reaction with CS_2 to give the analogous $RhCl(CS)(PPh_3)_2$ is more complicated than was first believed. If the reaction is carried out in neat CS_2, an intermediate species $RhCl(\eta^1\text{-SCS})(\eta^2\text{-}CS_2)(PPh_3)_2$ is isolated, which readily decomposes in more polar solvents ($CHCl_3$, MeOH) forming $RhCl(CS)(PPh_3)_2$ (for its structure, see section 2.7.2).

$RhCl(PPh_3)_3$ as a homogenous hydrogenation catalyst [44, 45, 52]. The mechanism of this reaction has been the source of controversy for many years. One interpretation of the catalytic cycle is shown in Figure 2.15; this concentrates on a route where hydride coordination occurs first, rather than alkene coordination, and in which dimeric species are unimportant. (Recent NMR study indicates the presence of binuclear dihydrides in low amount in the catalyst system [47].)

The initial catalytic step involves reversible binding of H_2 to afford a rather crowded 18-electron species $RhH_2Cl(PPh_3)_3$. The ^{31}P NMR spectrum at −25°C it consists of a doublet of doublets owing to the *trans* phosphorus atoms (P_A) and a doublet of triplets owing to the unique phosphorus (P_B) (Figure 2.15) [47]. On warming to room temperature, broadening occurs as a result of phosphine ligand exchange; the loss of the couplings involving P_B shows that this is the phosphine dissociating, forming a 16-electron species $RhH_2Cl(PPh_3)_2$ that can bind an alkene (again affording an 18-electron species). This dihydride can now transfer the hydrogens to the unsaturated linkage (any alkyl intermediate is presumably shortlived as spectroscopic measurements have failed to detect them); addition is stereospecifically *cis*. Once the alkane is eliminated, the resulting coordinatively unsaturated 14-electron $RhCl(PPh_3)_2$ can rapidly undergo oxidative addition with H_2 to regenerate the dihydride intermediate.

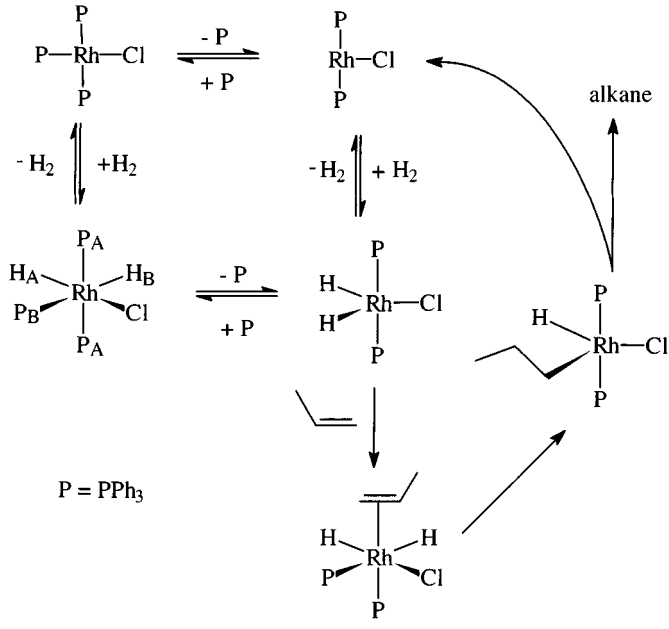

Figure 2.15 Cycle for the hydrogenation of alkenes catalysed by $RhCl(PPh_3)_3$.

Because the unsaturated hydrocarbon has to bind to rhodium in the presence of bulky PPh_3 groups, the catalyst favours unsubstituted double bonds ($RCH{=}CH_2$ rather than $RR^{I}C{=}CR^{II}R^{III}$). Since the alkyl intermediate is shortlived, there is little tendency to β-elimination with concomitant alkene isomerization. Although both alkene and alkyne functions are reduced, in general carbonyl or carboxylic groups and benzene rings are not, though aldehydes are frequently decarbonylated. Peroxides tend to oxidize and thus destroy the catalyst, so that substrates need to be purified carefully before use.

An example of a rhodium(I) complex with a tridentate phosphine is shown in Figure 2.16; it is formed by the usual route, reaction of the phosphine with $[RhCl(cycloocta\text{-}1.5\text{-}diene)]_2$.

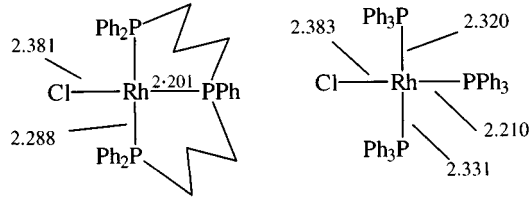

Figure 2.16 Bond lengths in a rhodium(I) complex of a tridentate phosphine compared with those in $RhCl(PPh_3)_3$.

It has an approximately square planar geometry, with bond lengths very similar to $RhCl(PPh_3)_3$ (Figure 2.5); like the latter, it undergoes a range of addition reactions, some involving no formal change in oxidation state, others a change to rhodium(III) species (Figure 2.17).

These are generally analogous to those of Wilkinson's compound, with the important difference that ligand dissociation cannot occur, so that the product of oxidative addition with H_2 cannot have a vacant site to bind an alkene and will thus not act as a hydrogenation catalyst [53].

4 : 1 complexes

The 4 : 1 complexes tend to be formed only by less bulky phosphines and even then tend to be coordinatively saturated.

$$RhCl(PPh_3)_3 \xrightarrow[X^-]{PR_3} Rh(PR_3)_4^+X^- \quad (X, \text{e.g. } PF_6, BF_4;\ PR_3 = PMe_3, PHPh_2)$$

Related compounds occur with bidentate phosphines

$$[RhCl(cod)]_2 \xrightarrow[X^-]{\text{diphos}} Rh(\text{diphos})_2^+X^-$$

(cod = cycloocta-1.5-diene; diphos = $Ph_2P(CH_2)_2PPh_2$, $Me_2P(CH_2)_2PMe_2$).

$Rh(Ph_2P(CH_2)_2PPh_2)_2^+ClO_4^-$ has essentially square planar coordination of rhodium (Rh–P 2.289–2.313 Å) [54].

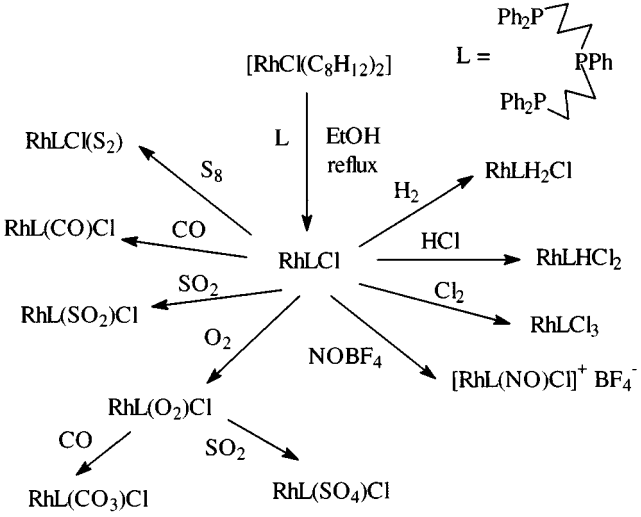

Figure 2.17 Reactions of the rhodium(I) complex of a tridentate phosphine.

5 : 1 complexes

Few of the 5:1 complexes [55] have been prepared, all with trialkylphosphites

$$[RhCl(cod)]_2 \xrightarrow{P(OR)_3} \{Rh[P(OR)_3]_5\}^+X^-$$

($X = BPh_4$, PF_6; R = Me, Et, Bu).

2.7.2 Carbonyl complexes

Three of the rhodium(I) carbonyl complexes are particularly important and are selected for special study.

$[RhCl(CO)_2]_2$

Reduction of hydrated $RhCl_3$ with CO at 100°C (best results are with CO saturated with methanol or ethanol) yields volatile red crystals of the dimer

$$RhCl_3.3H_2O \xrightarrow[100°C]{CO} [RhCl(CO)_2]_2$$

This has been shown to have an unusual dimeric structure (Figure 2.18) in which the two planar units are at an angle of 124° [56a].

The Rh–Rh distance is 3.12 Å, long compared with Rh–Rh single bonds (2.624 Å in $Rh_2(MeCN)_{10}^{4+}$, 2.73 Å in $Rh_4(CO)_{12}$); there is a weaker (3.31 Å) intermolecular attraction. Dipole moment and IR studies indicate that the structure is retained in solution and is, therefore, a consequence of electronic rather than solid-state packing effects. Furthermore, it is found for some other (but not all) $[RhCl(alkene)_2]_2$ and $[RhCl(CO)(PR_3)]_2$ systems. SCF MO calculations indicate that bending favours a Rh–Cl bonding interaction which also includes a contribution from Rh–Rh bonding [56b].

$[RhCl(CO)_2]_2$ undergoes a range of reactions (Figure 2.19) generally involving bridge cleavage and is, therefore, a useful starting material.

$RhH(CO)(PPh_3)_3$

$RhH(CO)(PPh_3)_3$ [57] is most conveniently prepared by

$$RhCl(CO)(PPh_3)_2 \xrightarrow[EtOH]{N_2H_4} RhH(CO)(PPh_3)_3$$

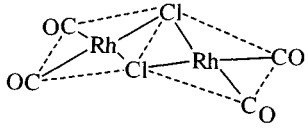

Figure 2.18 The structure of $[RhCl(CO)_2]_2$.

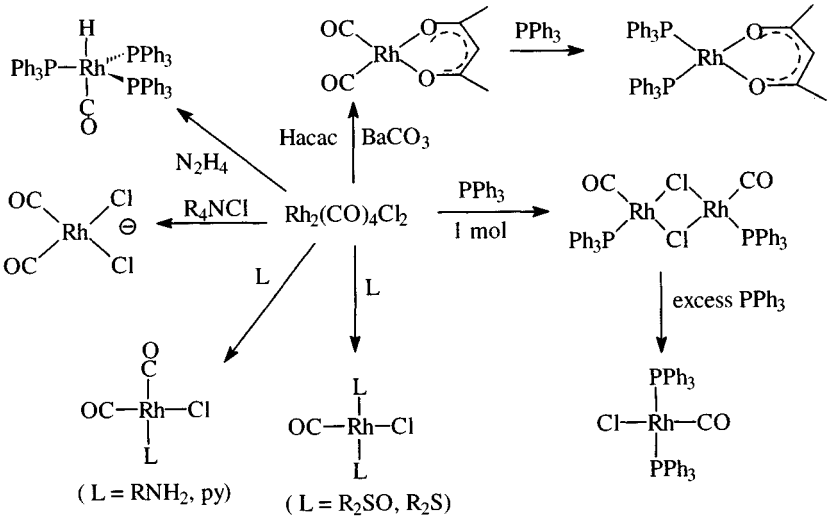

Figure 2.19 Reactions of $[RhCl(CO)_2]_2$.

It shows ν(Rh–H) and ν(C–O) at 2041 and 1918 cm^{-1}, respectively, in the IR spectrum (Nujol) and the low-frequency hydride resonance at $\delta = -9.30$ ppm in the ^1H NMR spectrum. It has a tbp structure (Figure 2.20) with the rhodium displaced out of the P_3 plane by 0.36 Å towards the CO.

It is an 18-electron species but in solution it tends to lose one PPh_3 to give $RhH(CO)(PPh_3)_2$, an active catalyst for hydroformylation and, to a lesser extent, hydrogenation of alkenes. (Evidence for the dissociation includes the fact that in the presence of other phosphines, mixed species $RhH(CO)(PPh_3)_2(PR_3)$ are formed by scrambling.) Initial coordination of the alkene is, in the absence of added CO, followed by hydrogenation (presumably via coordination of H_2 and an alkyl (intermediate)). Under a pressure of CO, hydroformylation occurs, with a high stereoselectivity in favour of straight-chain aldehydes, especially in the presence of added PPh_3. This supports the involvement of a crowded species (Figure 2.21) as the intermediate [58].

This process has been used commercially at the 100 kilotonne per year level running at around 100°C/20 atm.

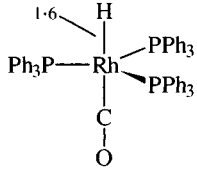

Figure 2.20 The structure of $RhH(CO)(PPh_3)_3$.

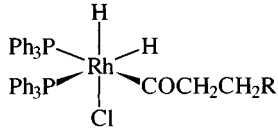

Figure 2.21 Probable structure of the intermediate in alkene hydroformylation catalysed by $RhH(CO)(PPh_3)_3$.

trans-RhCl(CO)(PPh$_3$)$_2$ and related compounds

trans-$RhCl(CO)(PPh_3)_2$ [59] is the rhodium analogue of 'Vaska's compound' (section 2.10.2) and undergoes analogous oxidative addition reactions. It is a yellow solid (IR ν(C–O) 1980 cm^{-1} ($CHCl_3$)) conveniently obtained by the following route using methanal as the source of the carbonyl group.

$$RhCl_3 \xrightarrow[\text{EtOH reflux}]{PPh_3/HCHO} RhCl(CO)(PPh_3)_2$$

The *trans*-geometry (confirmed by X-ray) keeps the bulky PPh_3 groups as far apart as possible (Figure 2.22).

Other $RhX(CO)(PPh_3)_2$ compounds can be made as shown in Figure 2.23; metathesis with an alkali metal halide or pseudohalide is often convenient, but the most versatile route, as with the iridium analogues, is a two-stage process in which the fluoro complex is first prepared, the fluorine then being readily displaced.

Attempted synthesis of $RhY(CO)(PPh_3)_2$ in undried solvents (Y = a weakly coordinating anion, e.g. BF_4, ClO_4, SO_3CF_3) leads to $[Rh(H_2O)(CO)(PPh_3)_2]^+Y^-$. The water molecule is bound sufficiently strongly not to be displaced by alkenes (ethene, phenylethanol) but is removed by pyridine or CO (at 1 atm) yielding $Rh(CO)_3(PPh_3)_2^+$.

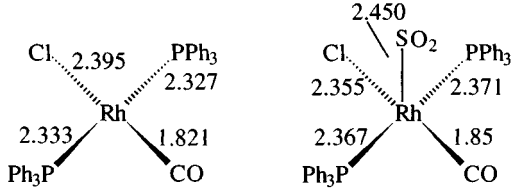

(X = Cl; Q = Ph)

X	Q	*n*	Rh–P	Rh–X	Rh–C
Cl	O	0	2.327–2.33	2.395	1.821
I	O	0	2.316–2.336	2.683	1.81
SH	O	0	2.314	2.416	1.767
Cl	S	0	2.335–2.337	2.386	1.787
OH_2	O	1	2.351	2.122	1.792

Figure 2.22 Bond lengths in $RhCl(CO)(PPh_3)_2$, $RhX(CQ)(PPh_3)_2$] and $[Rh(OH_2)(CO)(PPh_3)_2]^+$ as well as in the SO_2 adduct.

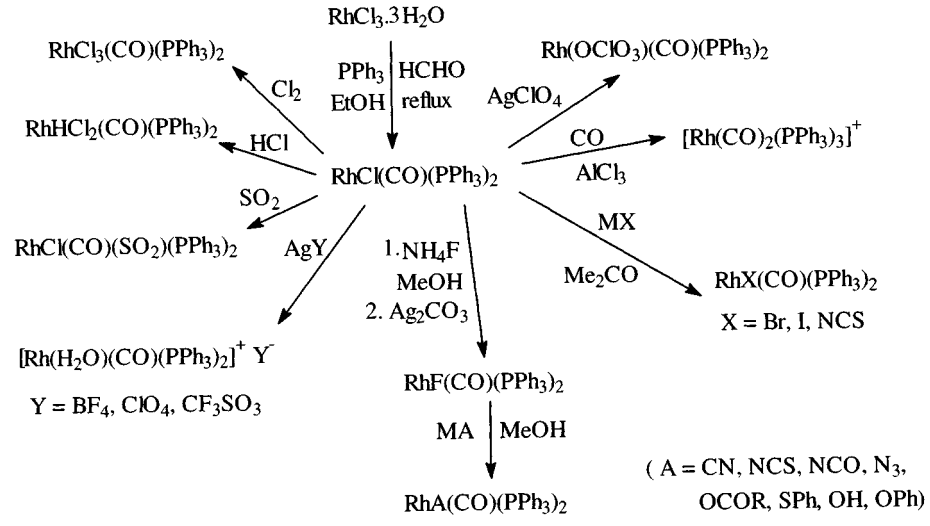

Figure 2.23 Reactions of $RhCl(CO)(PPh_3)_2$.

The mercapto complex $Rh(SH)(CO)(PPh_3)_2$ can be made by an unusual route [60] involving COS, where an intermediate with CS bound COS has been suggested.

$$RhH(PPh_3)_4 + COS \xrightarrow{\text{toluene}} Rh(\eta^2\text{-}COS)H(PPh_3)_3$$
$$\rightarrow Rh(SH)(CO)(PPh_3)_2 + 2PPh_3$$

The ^1H NMR spectrum of $Rh(SH)(CO)(PPh_3)_2$ in the mercaptide region (Figure 2.24) shows a 1:2:1 triplet owing to coupling to two equivalent (mutually *trans*) phosphines (J(P–H) 18.1 Hz), each line split into a doublet by a weaker coupling to ^{103}Rh (J(Rh–H) 1.6 Hz).

Structures have been determined for a number of these compounds, showing that the Rh–P bonds are little affected by the *cis*-ligands (Figure 2.22). The shorter Rh–C distance in the thiocarbonyl is probably a result of greater Rh=C back-bonding. Addition of SO_2 results in the formation of a 5-coordinate (sp) adduct with the expected lengthening in all bonds.

Other $RhCl(CO)(PR_3)_2$ compounds ($PR_3 = PEt_3$, PBu_3, $Palkyl_2Ph$, $PalkylPh_2$, $P(OR)_3$, PBu^t_2 alkyl) have been synthesized by the general route

$$[Rh(CO)_2Cl]_2 + 4PR_3 \xrightarrow{\text{MeOH}} 2RhCl(CO)(PR_3)_2 + 2CO$$

Structures have been determined for $PR_3 = PMe_2Ph$ and PBu^t_3 [61]. In the former, the square planar geometry is retained (with slightly shorter Rh–P bonds (2.316 Å) than for $PR_3 = PPh_3$), but in the latter, there is pronounced lengthening of the Rh–P bonds (Rh–Cl 2.395 Å, Rh–P 2.425-2.430 Å, Rh–C 1.784 Å) and a distortion towards a tetrahedral structure (P–Rh–P

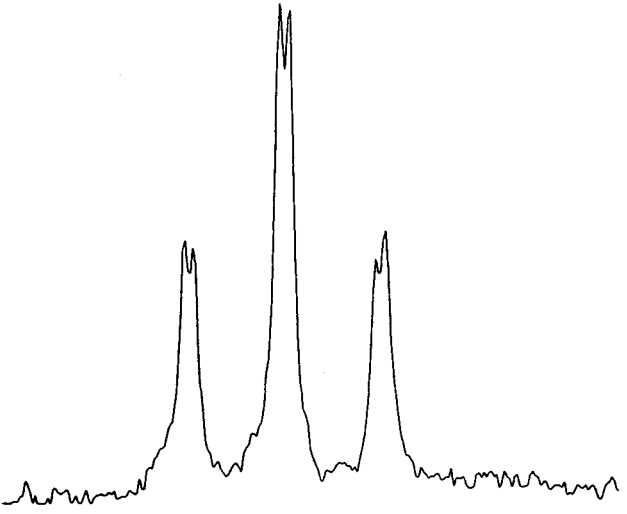

Figure 2.24 NMR spectrum of $Rh(SH)(CO)(PPh_3)_2$ in the mercaptide region. (Reprinted with permission from *Inorg. Chem.*, 1982, **21**, 2858. Copyright (1982) American Chemical Society.)

162.5°, C–Rh–Cl 150.7°) and some bending of the Rh–C–O bond (162.3°). Some short O–H and Cl–H intramolecular contacts may be responsible for the distortion though it has been suggested that in a distorted tetrahedral environment there may be an interaction between Rh d_{xz} electrons and the CO π^*-orbital causing bending.

Further evidence of steric crowding owing to bulky phosphines is found in $RhCl(CO)(PBu^t_2 alkyl)_2$. Study of the ^{31}P NMR spectra at low temperature, 'freezing in' the rotational conformers shows separate signals for each (Figure 2.25) [62].

$RhCl(CO)(PR_3)_2$ (R = Et, Me, Ph) and the corresponding iridium systems undergo UV photolysis with the loss of CO, generating short-lived $RhCl(PR_3)_2$ species that act as catalysts for alkane carbonylation. Thus photolysis for 16.5 h under 1 atm CO using $RhCl(CO)(PMe_3)_2$ in pentane gives 2725% hexanal with high regioselectivity (45 : 1 hexanal to 2-methylpentanal) [63].

The complexes $[RhCl(CO)(PR_3)]_2$ can exist as *cis*- and *trans*-isomers (Figure 2.26).

The *cis*-structure (like $[Rh(CO)_2Cl]_2$ folded, with an angle of 123°) has been confirmed for PMe_2Ph (X-ray) whereas the $P(NMe_2)_3$ analogue is *trans* (IR). Comparison of solid-state and solution IR spectra indicates that both isomers are present in solution ($PR_3 = PMe_3$, PMe_2Ph, $P(NMe_2)_3$) [64].

Anionic carbonyl complexes of both rhodium(I) and (III) are synthesized by decarbonylation of formic acid, with reduction to rhodium(I) occurring

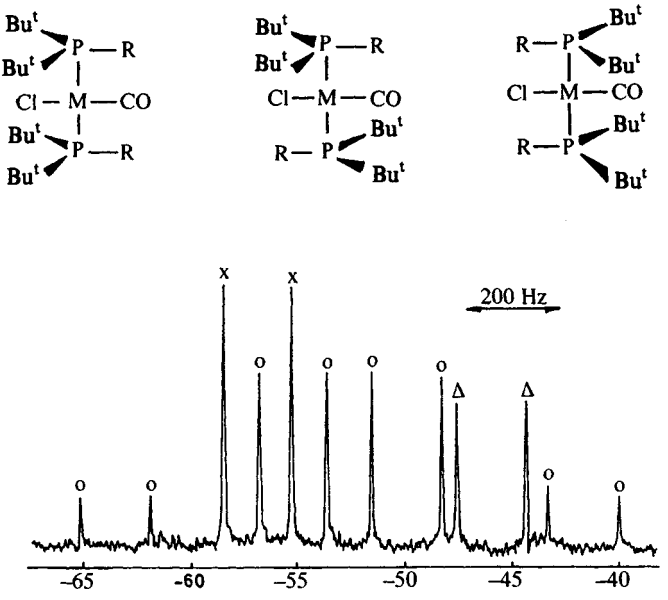

Figure 2.25 ^{31}P NMR spectrum of *trans*-$RhCl(CO)(PBu^t_2Et)_2$ at −60°C. The patterns ×, ○, △ correspond to the three conformers. (Reproduced with permission from *Chem. Comm.*, 1971, 1103.)

on extended reflux

$$RhX_3 \xrightarrow[\text{MX reflux}]{\text{HCOOH}} Rh(CO)X_5^{2-} \xrightarrow[\text{reflux}]{\text{HCOOH}} Rh(CO)_2X_2^-$$

Such a complex, *cis*-$Rh(CO)_2I_2^-$, is the active species in the Monsanto process for low-pressure carbonylation of methanol to ethanoic acid. The reaction is first order in iodomethane and in the rhodium catalyst; the rate-determining step is oxidative addition between these followed by

$$Rh(CO)_2I_2^- + MeI \Leftrightarrow Rh(CO)_2(Me)I_3^-$$

methyl migration generating $(MeCO)Rh(CO)I_3^-$. This can then add CO, eliminate MeCOI (subsequently hydrolysed to the acid) and regenerate $Rh(CO)_2I_2^-$.

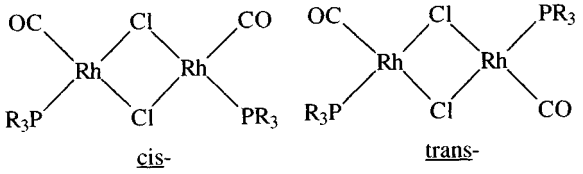

Figure 2.26 Isomers of $[RhCl(CO)(PR_3)]_2$.

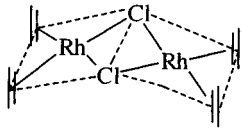

Figure 2.27 The structure of $[RhCl(C_2H_4)_2]_2$.

2.7.3 Alkene complexes

If ethene is bubbled through a methanolic solution of $RhCl_3.3H_2O$, red–orange crystals of $[RhCl(C_2H_4)_2]_2$ precipitate in a redox reaction.

$$2RhCl_3 + 6C_2H_4 + 2H_2O \rightarrow [RhCl(C_2H_4)_2]_2 + 2MeCHO + 4HCl$$

This has a 'folded' structure (Figure 2.27) similar to that of rhodium carbonyl chloride (Figure 2.18) with ethene acting as a two-electron donor, but ethene is more weakly held and readily displaced by CO and certain alkenes (e.g. cycloocta-1,5-diene).

Reaction under controlled conditions with tertiary phosphines leads to partial displacement of alkene retaining the dimeric structure [65].

Reaction of the dimer with Na(acac) leads to cleavage of the bridge giving yellow crystals of $Rh(alkene)_2(acac)$:

$$[RhCl(C_2H_4)_2]_2 + 2Na(acac) \rightarrow 2NaCl + 2(C_2H_5)Rh(acac)$$

C_2F_4 displaces one ethene to give $Rh(C_2H_4)(C_2F_4)(acac)$, as does hexafluorodewarbenzene, whereas other alkenes (e.g. propene, styrene, vinyl chloride) displace both ethenes. Comparison of the structures of two complexes (Figure 2.28) shows that the Rh–C bonds are shorter to tetrafluoroethene, because C_2F_4 is a better π-acceptor, with concomitant strengthening of the Rh–C bond.

NMR spectra show the ethene molecules to undergo a 'propeller' type rotation about the metal–alkene axis: the fluxionality is removed on cooling; such rotation is not observed with coordinated C_2F_4, indicating a higher barrier to rotation, in keeping with the stronger Rh–C bonds [66].

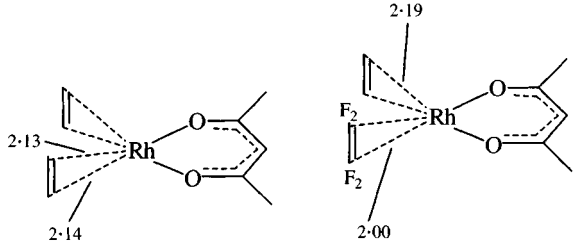

Figure 2.28 The structures of $Rh(acac)(C_2H_4)_2$ and $Rh(acac)(C_2H_4)(C_2F_4)$.

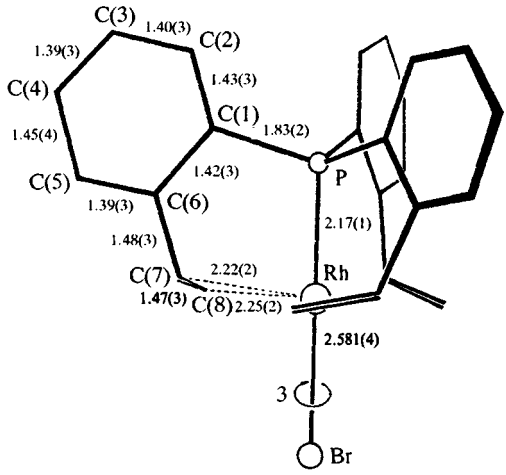

Figure 2.29 The structure of RhBr((*o*-vinylphenyl)$_3$P). (Reproduced with permission from *J. Chem. Soc., Dalton Trans.*, 1973, 2202.)

A number of tertiary phosphine ligands have been synthesized that also contain an alkene linkage capable of coordinating to a metal. A good example of this kind of coordination is formed in the complex of (tri-*o*-vinylphenyl)phosphine (Figure 2.29); with each alkene acting as a two-electron donor, a noble gas configuration is achieved [67].

2.7.4 Isocyanide complexes

Isocyanide complexes [68] can readily be prepared using excess isocyanide as the reducing agent:

$$[RhCl(CO)_2]_2 \xrightarrow[RNC]{\text{exc.}} Rh(RNC)_4^+ \xleftarrow[RNC]{\text{exc.}} RhCl_3.3H_2O$$

(R, e.g. alkyl, Ph)

In solution the compounds exhibit solvent-dependent colours; in dilute solution in non-polar solvents, planar monomers are present but in more concentrated solutions oligomerization occurs. In the solid state a dimeric structure has been identified (X-ray, Figure 2.30); with R = Ph there is a staggered configuration (Rh–Rh 3.193 Å) but with other isocyanides (R = 4-FC_6H_4) the configuration is eclipsed.

The weak Rh–Rh bond is taken to occur by d_{z^2}-d_{z^2} overlap.

Like other planar rhodium(I) complexes, $Rh(RNC)_4^+$ undergoes oxidative addition with halogens to form 18-electron rhodium(III) species and also add other small molecules (SO_2, NO^+) (Figure 2.31).

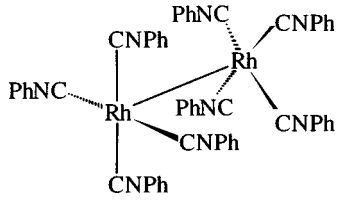

Figure 2.30 The dimeric structure of $[Rh_2(PhNC)_8]^{2+}$ in the solid state.

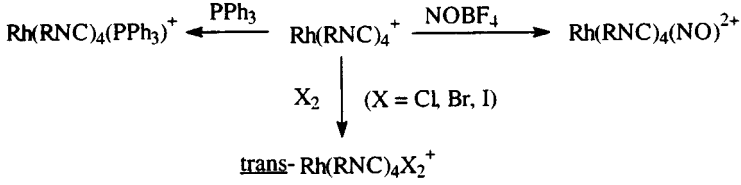

Figure 2.31 Reactions of $[Rh(RNC)_4]^+$.

2.8 Rhodium(II) complexes

Until recently, well-authenticated cases of the rhodium(II) oxidation state were rare, with the exception of the dinuclear carboxylates. They fall into two main classes, although there are other rhodium(II) complexes:

1. paramagnetic complexes ($4d^7$) with bulky phosphines, usually of the type $Rh(PR_3)_2X_2$
2. diamagnetic dinuclear carboxylates, and related dimers.

2.8.1 Phosphine complexes

Reaction of $RhCl_3.3H_2O$ with bulky tertiary phosphines at room temperature or below generally leads to reduction to rhodium(II).

$$RhCl_3.3H_2O \xrightarrow[0-25°C]{PR_3} \textit{trans}\text{-}RhCl_2(PR_3)_2$$

(PR_3 = P(*o*-tolyl)$_3$, Pcy_3, PBu^t_2R' (R' = Me, Et, Pr^n etc.).

Oxidative cleavage may be used

$$[RhX(Pcy_3)_2]_2 \xrightarrow{X_2} \textit{trans}\text{-}RhX_2(Pcy_3)_2 \qquad (X = Cl, Br)$$

(Other syntheses are mentioned in section 2.9.5.)

These compounds are paramagnetic (PR_3 = P(*o*-tolyl)$_3$, $\mu_{eff} = 2.3\,\mu_B$; $PR_3 = Pcy_3$, $\mu = 2.24\,\mu_B$), deeply coloured (usually blue–green) and have IR spectra resembling those of *trans*-$PdCl_2(PR_3)_2$ systems. The structure has been determined for $PR_3 = PPr^i_3$ (Rh–P 2.366 Å, Rh–Cl 2.298 Å) [69].

A more unusual complex is formed by the very bulky tris(2,4,6-trimethoxyphenyl)phosphine (tmpp) [70].

$$[Rh_2(MeCN)_{10}](BF_4)_4 \xrightarrow{tmpp} 2[Rh(tmmp)_2]^{2+} + 4BF_4^-$$

The complex ion (Figure 2.32) contains Rh_2^+ bound *cis* to two phosphorus atoms (2.216 Å) and more distantly to four oxygens (2.201–2.398 Å), exhibiting a distortion ascribed to the Jahn–Teller effect; it is paramagnetic ($\mu = 1.80\,\mu_B$) and exhibits an ESR spectrum (Figure 2.33) showing rhodium hyperfine coupling as the doublet for $g_{||}$.

The complex reacts with CO reversibly via a series of redox reactions. $Rh(TMPP)_2^{2+}$ forms adducts with bulky isocyanides RNC (R = Bu^t, Pr^i), retaining the +2 state but changing to a *trans*-geometry (Figure 2.34) with monodentate phosphines (and uncoordinated ethers) (R = Bu^t, $\mu_{eff} = 2.04\,\mu_B$; $g_\perp = 2.45$, $g_{||} = 1.96$).

2.8.2 Dimers

The second class of rhodium(II) complexes is the dimers [71]. The dimeric

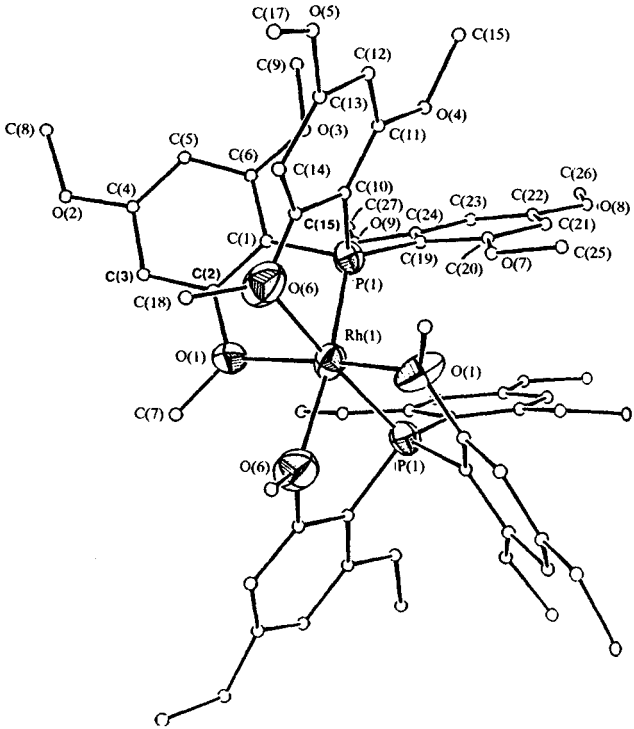

Figure 2.32 The structure of $[Rh(tmpp)_2]^{2+}$. (Reprinted with permission from *J. Am. Chem. Soc.*, 1991, **111**, 5504. Copyright (1991) American Chemical Society.)

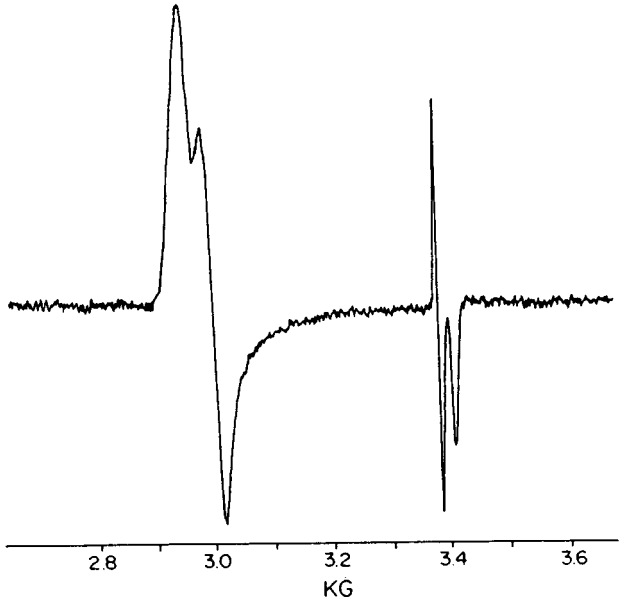

Figure 2.33 The ESR spectrum of $[Rh(tmpp)_2]^{2+}$ in CH_2Cl_2/toluene at 8 K. (Reprinted with permission from *J. Am. Chem. Soc.*, 1991, **111**, 5504. Copyright (1991) American Chemical Society.)

acetate can conveniently be prepared as a green methanol solvate:

$$RhCl_3.xH_2O \xrightarrow[\text{MeCH reflux}]{\text{MeCOOH/MeCOONa}} Rh_2(OCOMe)_4.2MeOH$$

The methanol can be removed by heating gently *in vacuo*. Similar compounds can be made with other carboxylate groups, either by using this method or by heating the acetate with excess carboxylic acid. Treatment of the anhydrous carboxylate with various neutral ligands (L) or anionic donors (X^-) forms $Rh_2(OCOR)_4L_2$ and $[Rh_2(OCOR)_4X_2]^{2-}$, respectively. The colour of the adduct depends on the donor atom in L (or X):

blue to green: oxygen
pink to red: nitrogen
orange to brown–red: phosphorus or sulphur.

These compounds all have the 'lantern' structure shown in Figure 2.35.

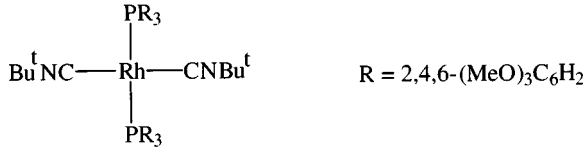

Figure 2.34 Isocyanide adducts of $[Rh(tmpp)_2]^{2+}$.

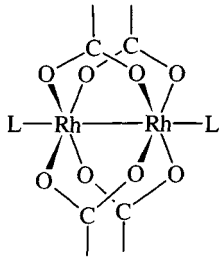

Figure 2.35 The 'lantern' structure adopted by dimeric rhodium(II) carboxylates.

Structural data for many carboxylates (Table 2.3) consistently show the presence of a metal–metal bond around 2.4 Å, shorter than that in rhodium metal (2.7 Å).

There is a slight dependence on the nature of the carboxylate group and upon the axial ligand, but they are not imposed by the steric requirements of the carboxylates. Some points are germane to this:

1. Adducts are formed with hard and soft donors, including π-acids such as CO, PF_3 and PPh_3. DMSO bonds through S for R = Me and Et, but through O when R = CF_3.

Table 2.3 Bond lengths in rhodium(II) carboxylates (Å)

(a) $Rh_2(OCOMe)_4L_2$

L	Rh–Rh	Rh–L
MeOH	2.377	2.286
MeCN	2.384	2.254
H_2O	2.3855	2.310
py	2.399	2.227
Me_2SO	2.406	2.451
$P(OMe)_3$	2.4556	2.437
$P(OPh)_3$	2.445	2.418
PPh_3	2.4505	2.477
PF_3	2.4215	2.340
CO	2.4193	2.091
Cl^-	2.3959	2.585
PhSH	2.4024	2.548
$AsPh_3$	2.427	2.576

(b) $Rh_2(OCOR)_4(H_2O)_2$

R	Rh–Rh	Rh–OH_2
Me	2.3855	2.310
CMe_3	2.371	2.295
CF_3	2.394	2.243

2. The long Rh–P bonds in the tertiary phosphine adducts show little dependence upon the tertiary phosphine and are interpreted in terms of a largely σ-component in the Rh–P bond; they are also affected by the strong *trans*-influence of the Rh–Rh bond.
3. ESCA data support a rhodium(II) oxidation state in these compounds. Therefore, the Rh $3d_{5/2}$ binding energy is *c.* 309.2 eV in simple carboxylates, midway between those in typical rhodium(I) complexes (*c.* 308.5 eV) and rhodium(III) complexes (*c.* 310.7 eV) [72].
4. The diamagnetism of all these rhodium(II) compounds indicates spin pairing via a metal–metal bond.
5. The lantern structure is quite stable, unlike certain other Rh_2 dimers. Protonation was formerly claimed to give 'Rh_2^{4+}' aqua ions, but they are believed now to be $[Rh_2(OCOMe)_3]^+$ (aq.) and $[Rh_2(OCOMe)_2]^{2+}$ (aq.) [73].
6. One-electron oxidation to $[Rh_2(OCOMe)_4(H_2O)_2]^+$ leads to an ion (violet to orange, depending on solvent) with a shorter Rh–Rh bond (2.317 Å) than that in the neutral molecule (2.385 Å), suggesting the electron has been removed from an orbital with anti-bonding character.

Unsolvated $[Rh_2(OCOR)_4]_2$ can be obtained by sublimation. The 'lantern' structure is retained with the axial position occupied by oxygens from neighbouring dimer units. The presence of axial ligands has little effect on the Rh–Rh bond; therefore, in $[Rh_2(OCOCF_3)_4]$ Rh–Rh is 2.382 Å compared with 2.394 Å in $[Rh_2(OCOCF_3)_4(H_2O_2)]$ and 2.418 Å in $Rh_2(OCOCF_3)_4(MeCN)_2$ [74].

The assignment of the Rh–Rh stretching frequency in the vibrational spectra of these compounds has been controversial for some 20 years, with ν(Rh–Rh) assigned variously to bands in the 150–170 and 280–350 cm^{-1} regions. Recent resonance Raman studies (Figure 2.36) exciting the metal-based $\sigma \rightarrow \sigma^*$ transition in $Rh_2(OCOMe)_4(PPh_3)_2$ showed enhancement of the symmetric stretching mode, at 289 cm^{-1}.

Isotopic (^2H, ^{18}O) labelling of the carboxylate groups has virtually no effect, as expected, on this band but produces shifts of 6–14 cm^{-1} in bands at 321 and 338 cm^{-1}, showing them to arise from Rh–O stretching [75].

Complexes of thiocarboxylic acids, $Rh_2(SCOR)_4L_2$, similarly adopt the 'lantern' structure. Rh–Rh distances are significantly greater than in the analogous carboxylates (R = Me_3C, L = py, Rh–Rh 2.514 Å; R = Ph, L = py, Rh–Rh 2.521 Å; R = Me_3C, L = PPh_3, Rh–Rh 2.584 Å). Raman studies on $Rh_2(SCOMe)_4L_2$ (L = PPh_3, $AsPh_3$, $SbPh_3$, MeCOSH) assign ν(Rh–Rh) to bands in the region of 226–251 cm^{-1}, significantly lower than in the carboxylates, consistent with the longer and weaker Rh–Rh bond [76].

Part of the upsurge in interest in rhodium(II) carboxylates since the early 1970s results from the discovery that they have potential as anti-tumour

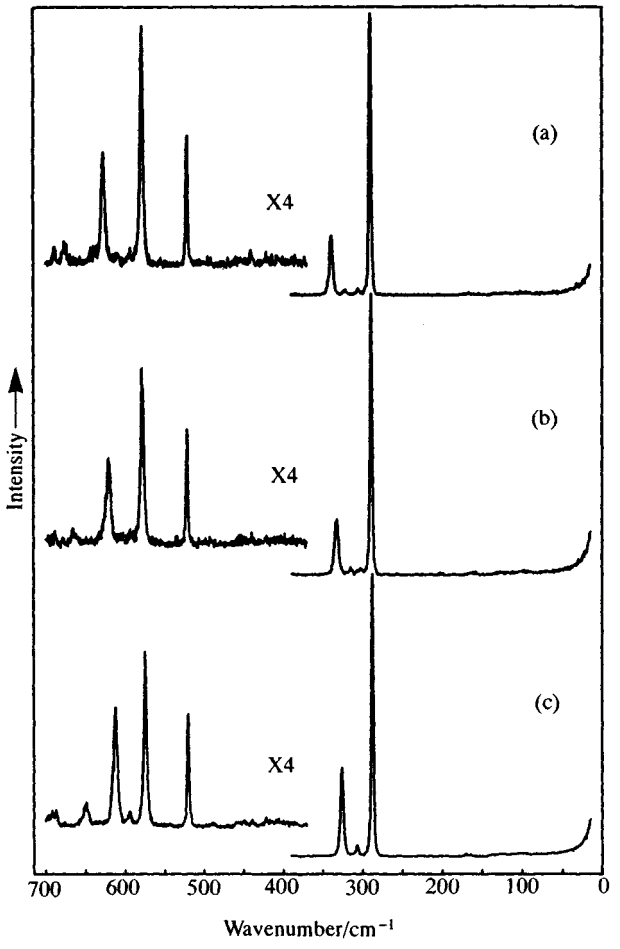

Figure 2.36 Resonance Raman spectra of (a) $Rh_2(^{16}O_2)CMe_4(PPh_3)_2$; (b) $Rh_2(^{18}O_2)CMe_4(PPh_3)_2$; (c) $Rh_2(^{16}O_2)C(CD_3)_4(PPh_3)_2$. Recorded as KCl discs at 80 K, L = 363.8 nm. (Reprinted with permission from *J. Am. Chem. Soc.*, 1986, **108**, 518. Copyright (1986) American Chemical Society.)

agents. The dimers form adducts with many biologically important N-donors but react irreversibly with some compounds containing SH groups. It seems that they may inhibit DNA synthesis by deactivating sulphydryl-containing enzymes [77].

Bonding in the dimers

Several MO schemes are suggested, most with a single bond but differing to some extent on the ordering of the energy levels [78] (Figures 2.37 and 2.38). The most recent results indicate the highest occupied MO (HOMO) is of σ-symmetry, consistent with ESR results on $[Rh_2(OCOR)_4(PR_3)_2]^+$.

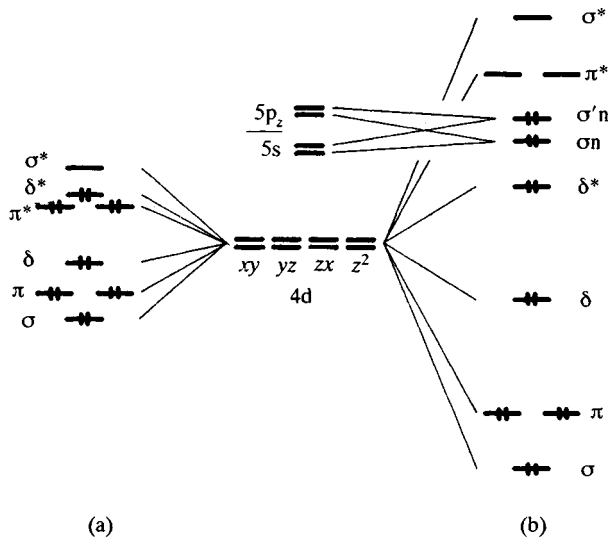

Figure 2.37 Models for the metal–metal bonding in $Rh_2(O_2CR)_4$. (a) corresponds to a single-bond; (b) corresponds to a triple-bond model in which there is a greater interaction between the rhodium 4d orbitals than between the 4d and 5s, 5p manifolds. (Reprinted with permission from *J. Am. Chem. Soc.*, 1981, **103**, 364. Copyright (1981) American Chemical Society.)

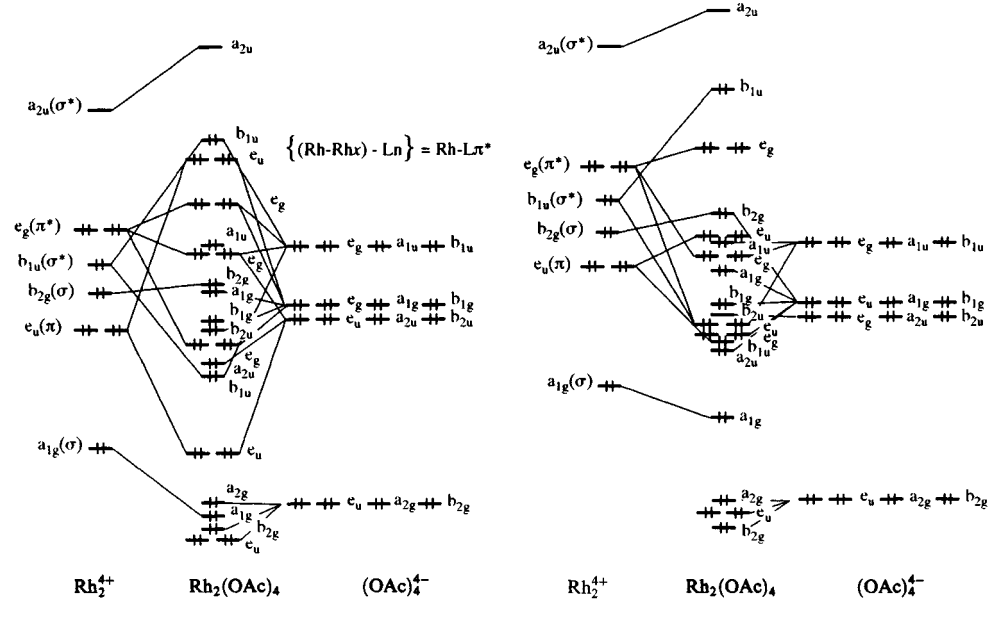

Figure 2.38 The effect of varying the relative energies of the metal and ligand orbitals upon the final molecular orbital scheme for a dimeric rhodium carboxylate. (Reprinted from *Coord. Chem. Rev.*, **50**, 109, 1983, with kind permission from Elsevier Science S.A., P.O. Box 564, 1001 Lausanne, Switzerland.)

In the MO scheme the rhodium atoms use their $d_{x^2-y^2}$ orbitals to form the Rh–O bonds, the remaining 4d orbitals are used to form four pairs of bonding and anti-bonding MOs (σ, δ and π) (Figure 2.37a).

The ligands interact with the two orbitals of σ-symmetry modifying the ordering somewhat (Figure 2.37b). As has been pointed out, altering the relative positions of the metal orbitals relative to those of the carboxylates affects the final scheme considerably (Figure 2.38).

Other compounds with the lantern structure include the acetamidates $Rh_2(MeCONH)_4L_2$ and the mixed-valence anilinopyridinate $Rh_2(ap)_4Cl$ (Figure 2.39), which has an unusual ESR spectrum in that the electron is localized on one rhodium [79].

Bridging ligands are not essential for the stability of dimers. Reduction of $[Rh(H_2O)_5Cl]^{2+}$ is believed to give a dimer $[Rh_2(H_2O)_{10}]^{2+}$.

Extended reflux of a MeCN solution of $Rh_2(OCOMe)_4$ with excess $Et_3O^+BF_4^-$ leads to successive replacement of the acetates [80]:

$$Rh_2(OCOMe)_4 \rightarrow [Rh_2(OCOMe)_2(MeCN)_6]^{2+} \rightarrow [Rh_2(MeCN)_{10}]^{4+}$$

$[Rh_2(MeCN)_{10}]^{4+}$ has a staggered structure (minimizing inter-ligand repulsions) with a Rh–Rh distance of 2.624 Å (presumably corresponding to a Rh–Rh single bond uninfluenced by bridging ligands (Figure 2.40).

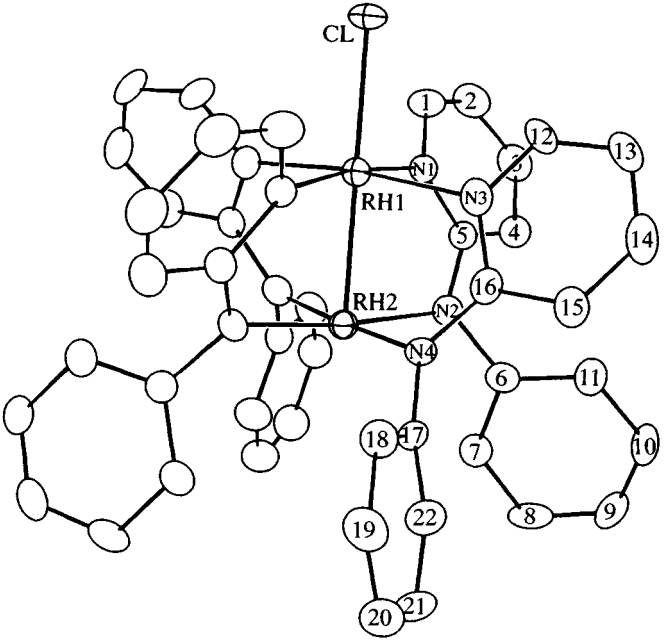

Figure 2.39 The 'lantern' structure of the dimeric rhodium antipyrine complex $Rh_2(ap)_4Cl$. (Reprinted with permission from *Inorg. Chem.*, 1988, **27**, 3783. Copyright (1988) American Chemical Society.)

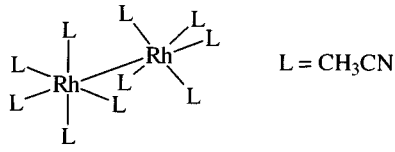

Figure 2.40 The staggered structure of the dimeric ion $[Rh_2(MeCN)_{10}]^{2+}$.

Reaction of $Rh_2(OCOR)_4$ with dimethylglyoxime leads to a non-bridged dimer [81].

$$Rh_2(OCOMe)_4 \xrightarrow{DMGH} Rh_2(DMG)_4$$

The bis(PPh_3) adduct has a long Rh–Rh bond of 2.936 Å, whereas in the 'mixed' dimer $Rh_2(OCOMe)_2(DMG)_2(PPh_3)_2$ where only two acetates bridge, Rh–Rh is 2.618 Å (Figure 2.41).

2.8.3 Other complexes

Photolysis of the rhodium(III) complex of octaethylporphyrin gives a rhodium(II) dimer that readily undergoes addition reactions to afford rhodium(III) species (Figure 2.42).

With more bulky porphyrins like TMP, a stable low-spin monomer Rh(TMP) can be isolated ($g_\perp = 2.65$, $g_{||} = 1.915$), which forms a paramagnetic CO adduct.

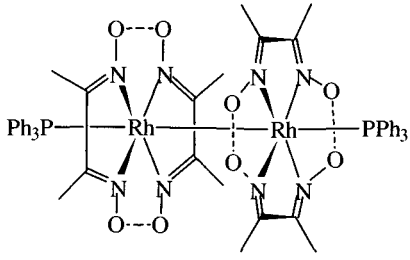

Figure 2.41 A dimeric non-bridged rhodium dimethylglyoxime complex (for clarity the hydrogen atoms in the hydrogen bonds are not shown).

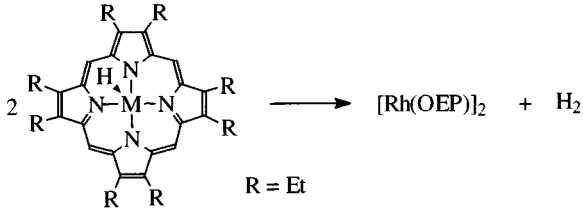

Figure 2.42 Synthesis of a dimeric rhodium(II) octaethylporphyrin complex.

A number of rhodium(III) complexes of thiacrown ligands can be reduced to give rhodium(II) species identifiable in solution. Thus controlled potential electrolysis of $Rh(9S_3)_2^{3+}$ ($9S_3$ = 1,4,7-trithiacyclononane) gives $Rh(9S_3)_2^{2+}$ ($g_1 = 2.085$, $g_2 = 2.042$, $g_3 = 2.009$) [82].

2.9 Rhodium(III) complexes

A considerable number of rhodium(III) complexes exist. Their stability and inertness are as expected for a low-spin d^6 ion; any substitution leads to a considerable loss of ligand-field stabilization.

2.9.1 Complexes of O-donors

The yellow acetylacetonate contains octahedrally coordinated rhodium (Rh–O 1.992 Å; O–Rh–O 95.3°) [83].

$$Rh(NO_3)_3 \xrightarrow[pH\,7]{acac^-} Rh(acac)_3$$

The corresponding tri- and hexa-fluoroacetylacetonates may be similarly prepared. The stability of the acetylacetonate is such that not only can it be resolved on passage through a column of D-lactose, but the enantiomers retain their integrity on nitration or bromination.

Extended refluxing of hydrated $RhCl_3$ with excess oxalate leads to the tris complex, the potassium salt crystallizing as orange–red crystals with Rh–O 2.000–2.046 Å.

$$RhCl_3.3H_2O \xrightarrow[reflux,\,6\,h]{aq.\,K_2C_2O_4\,(6\,mol)} K_3Rh(C_2O_4)_3.4\tfrac{1}{2}H_2O$$

$Rh(C_2O_4)_3^{3-}$ was resolved by Werner as the strychnine salt but other ions, such as $Coen_3^{3+}$ and $Niphen_3^{3+}$, have been used more regularly for this [84].

The dinuclear rhodium(II) acetate is described in section 2.8.2; the dinuclear structure is retained on one-electron oxidation, but when ozone is used as the oxidant, a compound with a trinuclear Rh_3O core is formed, analogous to those formed by Fe, Cr, Mn and Ru. (It can also be made directly from $RhCl_3$.)

$$RhCl_3.3H_2O \xrightarrow[2.\,ClO_4^-]{1.\,MeCOOAg} [Rh_3O(O_2CMe)_6(H_2O)_3]^+ClO_4^-$$

$$Rh_2(O_2CMe)_4 \xrightarrow[2.\,ClO_4^-]{1.\,O_3/boiling\,MeCOOH} [Rh_3O(O_2CMe)_6(H_2O)_3]^+ClO_4^-$$

Rhodium forms an EDTA complex isomorphous with the corresponding ones of Ru, Fe, Ga and Cr. In Rh(EDTAH)(H_2O) one carboxylate is protonated and thus the acid is pentadentate, the water molecule completing the octahedron (Figure 2.43).

Next Page